Biomechanical Analyses of Oropharyngeal Swallowing

Mark A. Nicosia, Ahmed El-Sayed, Eric W. Nicosia, Ryan Young
Widener University, School of Engineering
One University Place, Chester, PA 19013
manicosia, ammamounel-sayed, ewnicosia, rmyoung8628@mail.widener.edu

Abstract

The transport of an ingested food "bolus" through the oropharynx is primarily a mechanical process, in which bolus flow characteristics are determined by relationships among the physical properties of the bolus, the propulsive forces applied by the oropharyngeal musculature, and the biomechanical measures utilized to protect the airway. It naturally follows that the application of tools from mechanics and modeling may offer the ability to enhance our understanding of normal physiological processes as well as optimize the use of diagnostic and therapeutic tools.

This paper focuses on two aspects of our work in oropharyngeal swallowing mechanics (1) developing numerical tools for improved modeling of oropharyngeal fluid dynamics and (2) development and application of an experimental system, consisting of a fluid bolus contained in the central groove of a simulated tongue, to validate the model. Preliminary data and future directions are discussed.

Keywords: oropharyngeal fluid mechanics, finite element method.

1. Introduction

The flow of a bolus through the oropharynx during a normal swallow is a complex mechanical process, and the successful passage of the bolus into the esophagus depends upon a myriad of factors, including the propulsive activity of the lingual and oropharyngeal musculature, the rheological properties of the bolus, and the airway protection measures. Consequently, many therapeutic strategies for swallowing disorders are mechanical in nature, such as: (1) texture modification, in which bolus material properties are altered to optimize bolus flow through the oropharyngeal cavity, or (2) postural changes, such as a chin tuck in which the chin is tucked into the chest during the swallow to open the vallecular space to contain more fluid. It naturally follows that the application of tools from mechanics may offer the ability to enhance our understanding of normal physiological processes as well as optimize the use of diagnostic and therapeutic tools.

Computer modeling is one such tool from mechanics which has been utilized in many physiological systems, but has not been extensively applied to oropharyngeal swallowing. Computer models of swallowing have the potential to predict bolus flow characteristics in response to given alterations in input parameters, such as bolus physical properties (such as in texture modification) or oropharyngeal geometry (such as in postural modifications).

The long-term goal of the work described here is to develop, validate, and apply numerical modeling tools to study normal and abnormal oropharyngeal bolus flow as well as to provide insight into diagnostic and therapeutic procedures. This paper provides an overview of the current state of the project, which is ongoing. We will describe two related aspects: (1) development of the numerical tools to simulate the complex process of oropharyngeal bolus flow, and (2) development an experimental apparatus for validation of the computer model that is relevant to swallowing and may also provide insights into oropharyngeal fluid mechanics.

Section 2 will provide a brief overview of the physiology of swallowing. This is followed in Section 3 by a brief review of relevant numerical methods for simulation of fluid-mechanics problems involving moving boundary and/or free-surfaces. In Section 4, we present the numerical method developed in this work, as well as its validation with a simple "sloshing tank" example. Section 5 describes the design, construction of an experimental apparatus to validate the computer model as well as some preliminary data. Finally, Section 6 describes ongoing and future work.

2. Physiological Background

In the United States alone, 15-30 % of the 44 million individuals currently over the age of 60 are estimated to have dysphagia (a general term for swallowing disorders), along with an estimated 50 % of nursing home patients. Swallowing disorders can have a profound effect on an individual's quality of life and can pose significant health

OPAL-09, June 26-27, 2009, Vancouver, BC, CA

risks, such as aspiration pneumonia, in which ingested material enters the trachea and lungs rather than the esophagus and gastrointestinal tract, leading to infection. Aspiration pneumonia is a serious and often life-threatening health concern for the institutionalized and hospitalized geriatric population.

In the typical configuration before a bolus is ejected from the oral cavity, termed the bolus containment phase, the tongue is cupped, with the tip against the front teeth and the back elevated against the soft palate. When a swallow is initiated, the tongue makes sequential (anterior-to-posterior) contact with the roof of the mouth, forming a stripping wave to propel the bolus. Nearly coincidently, the back of the tongue separates from the palate, allowing passage of the bolus into the pharynx. During a normal swallow, these actions are coordinated with several mechanisms which provide protection to the airway, including posterior, anterior motion of the hyolaryngeal complex, approximation of the vocal folds, and closure of the laryngeal vestibule.

Indeed, the passageway traversed by the bolus is coincident with the airway until the two separate at the level of the larynx. Thus, for the swallow to be safely executed, the airway must be quickly and transiently reconfigured to allow bolus flow into the esophagus, while simultaneously protecting the airway against invasion – whether it occurs before, during, or after a swallow.

As noted earlier, swallowing disorders, including aspiration, become more prevalent with increased age. As an individual ages, one of the normal changes that occurs in the oropharyngeal swallow is the development of a delay between the time that a bolus enters the pharynx and the onset of airway protection measures. Such a delay may lead to a portion of the bolus assuming a position in close proximity to an unprotected airway, leading to the potential for aspiration. This entry of the bolus into the pharynx prior to the onset of airway protection is sometimes referred to as "premature spillage."

Although there are many different behaviors associated with dysphagia, our initial focus is on bolus containment – that is, the prevention of premature spillage in response to lingual motions. The numerical and experimental procedures are focused on this phenomena – however, once developed and validated, they will have broad applicability to swallowing physiology and pathophysiology.

3. Numerical Modeling Techniques

3.1 Physical considerations

While there may be great benefit in the application of computer modeling to oropharyngeal bolus flow dynamics, there are also many challenges. On one hand, there are many mechanical issues involved which complicate such an analysis. The flow of a liquid bolus through the oropharyngeal chamber may be described as the highly transient flow of an air-fluid mixture through a complex three-dimensional geometry with time-dependent boundaries. Furthermore, for all but the simplest liquids, the bolus is composed of a rheologically complex material, potentially exhibiting nonlinear, viscoelastic material properties that are temperature-, time-, and shear-rate dependent. Finally, as it progresses through the oropharyngeal chamber, the bolus undergoes large displacements as well as large deformations.

Another computational issue that bears discussion is the question of the proper boundary condition at the interface between the tongue and the bolus. The classic boundary condition for simulation of viscous fluid flow is the "no-slip" condition. A different condition is often used in the case of lubricated flow, termed perfect slip, in which the wall shear stress is zero. For normal human swallowing, the presence of saliva lining the oral cavity likely renders the actual boundary condition somewhere between these two extremes. Note that the presence or absence of wall shear can profoundly influence the distribution of internal stresses within a material.

In addition to the purely numerical issues described in the previous paragraphs, oropharyngeal bolus flow mechanics are also characterized by a high degree of variability. One source of this variability derives from the kinematics of the tongue. During the oral stage of swallowing (including bolus ejection from the oral cavity), the tongue is a primary source of propulsion for the bolus. In a study by Tasko et al. [8], small pellets were attached to the surface of the tongue and tracked during 2 and 10 mL liquid swallows using the x-ray microbeam facility at the University of Wisconsin. The authors concluded that due to the high variability that was observed, they could not define a "low dimension quantitative description of the tongue kinematics during liquid swallowing"[8]. These data suggest that there may not be a unique pattern of lingual kinematics which is required for a successful swallow. This is not surprising, given that the tongue is under volitional control, and has a high number of degrees of freedom. In addition to this variability inherent in the physiological system, multiple studies point out the high degree of variability in what is input to the system – i.e., variability in rheological properties of a bolus (e.g., see [9]). Thus, to be of any predictive value, the results of any numerical model must address these potential sources of variability.

3.2 Numerical considerations

There are two frames of reference commonly utilized in computational mechanics, Eulerian and Lagrangian [1]. Fluid mechanics simulations are typically carried out in an Eulerian frame of reference, in which the flow of material through a fixed region of space is studied. In contrast, solid mechanics simulations are typically carried out in a

Lagrangian frame of reference, in which a fixed quantity of material is followed as it deforms under the action of applied loads. There are cases, however, in which it is advantageous to utilize a Lagrangian representation for a fluid mechanics problem – such as the transport of a fixed quantity of fluid through a system, as in oropharyngeal bolus transport. Such cases often involve moving boundaries and/or free surfaces. In the Lagrangian case, the boundaries stay well defined as the grid deforms since boundaries of the domain coincide with the element boundaries. This makes the application of boundary conditions or the tracking of a free surface straightforward. However, when the deformations become too severe, the underlying grid becomes distorted, leading to numerical inaccuracies, and eventually, termination of the simulation (if, for example, elements "turn inside out"). There are several methods that have been developed to address free surface flows, as briefly described below.

3.2.1 Eulerian methods

Eulerian methods have been developed to simulate free-surface flows on a fixed mesh, such as the Volume of Fluid Method. In these methods, a scalar function *F,* is defined for each cell in the grid. For each cell *F* ranges between 0 (no fluid in the cell) and 1 (cell completely full of fluid). An evolution equation for *F* is solved along with mass and momentum conservation equations as part of the numerical solution. In these methods, because the free surface does not necessarily correspond to element boundaries (*F* between 0 and 1 implies that a cell is partially full), it can be smeared, causing inaccuracies in its detection.

3.2.2 Moving Mesh Methods

A hybrid computational strategy has been developed to account for the large grid distortions associated with Lagrangian simulation, termed Arbitrary Lagrangian-Eulerian [2]. In this case, a Lagrangian simulation is run for either a fixed number of steps, or until the elements become too distorted. At this point the model is smoothed and the dependent variables are interpolated from the old, distorted grid to the new grid, at which time the Lagrangian simulation resumes. Usually, the mesh is not completely reformulated – rather the existing nodes are moved without changing the overall topology of the mesh. For example, in the pseudo-solid method, the domain is treated as an elastic solid, and the equations of elasticity are used to smooth the mesh. The interpolation algorithms, which are typically the most inaccurate aspect of these methods, are often referred to as "advection algorithms" in the literature, because the grid is seen to move through the fluid. Although these methods are powerful when moderate grid deformations are involved, they cannot handle the extremely large distortions typically inherent in Lagrangian fluid mechanics simulations, and the grid must be completely reformulated.

If the mesh is to completely reformulated, a commonly used automatic mesh generation method is the advancing front method, based on Delaunay triangulation. In this method, based on knowledge of ordered sets of boundary segments for the domain, a series of triangular elements are developed and gradually refined until a final mesh is converged upon. Since the position of internal nodes is not specified, nodal points will have moved after the re-mesh; in general there may be a different number of nodes before and after the remap. This necessitates an interpolation step to compute values of the dependent variables at the new grid locations.

3.2.3 Particle Methods

An alternative to methods that require a mesh is the class of methods termed "particle methods." In these methods, the continuum domain is represented by a set of points, where each point is imparted with a certain mass; dependent variables, such as velocity and density, are carried by the particles. One very powerful advantage associated with these methods is the lack of a need to maintain a predetermined connectivity between points; such connectivity is implied for a finite element mesh. This allows for a natural handling of the extremely large distortions that accompany fluid flows. However, an accurate representation of the boundary of the domain is sacrificed, which leads to challenges in both tracking the free surface of a flow and in the application of boundary conditions. Furthermore, although particle methods have been applied to viscoelastic flows, these are not yet commonplace.

4. Methods

4.1 General Overview

Based on the concepts described in the previous sections, we chose to build our numerical model using a Lagrangian method with adaptive re-meshing when the grid becomes distorted. We will first describe the development and validation of the basic Lagrangian method, followed by implementation and validation of the re-meshing algorithm. General information on the finite element method can be found in reference [3].

4.2 Numerical Model: Lagrangian Method

An updated Lagrangian formulation was utilized. In contrast to a total Lagrangian formulation, in which the reference configuration is unchanged over the course of the simulation, an updated Lagrangian formulation uses the previous time step as the reference configuration for each time step.

In this frame, the equations of mass and momentum conservation are given by,

$$\rho \dot{\mathbf{v}} = \nabla \bullet \boldsymbol{\sigma} + \rho \mathbf{f} \sigma \quad (1)$$

$$J = \frac{\rho_o}{\rho} = \frac{V}{V_o} \quad (2)$$

where J is the determinant of the deformation gradient tensor, $\mathbf{v}$ is the velocity vector, $\boldsymbol{\sigma}$ is the Cauchy stress tensor, $\mathbf{f}$ is the body force vector, and ∇ is the gradient operator. In the current simulations, gravity is included as a body force. Note that Equation (2) is not the common form of mass conservation used in fluid mechanics simulations – this point will be returned to later.

Boundary conditions are given by,

$$\boldsymbol{\sigma n} = \boldsymbol{\tau} \quad \text{on } \Gamma_\tau \quad (3)$$

$$\mathbf{x}(\mathbf{X},t) = \mathbf{D}(\mathbf{X},t) \quad \text{on } \Gamma_x, \quad (4)$$

where $\boldsymbol{\tau}$ is an applied surface traction, applied over the portion of the boundary given by Γ_τ, and $\mathbf{D}$ is a displacement boundary condition, applied over Γ_x.

Taking the scalar product of Eq. (1) with a virtual displacement, $\delta\mathbf{x}$, integrating over the volume, incorporating (3), and invoking the divergence theorem yields the weak form,

$$\int_\Omega \left(\rho \dot{\mathbf{v}} \bullet \delta\mathbf{x} + \sigma \bullet \nabla \delta\mathbf{x}\right) d\Omega - \int_{\Gamma_\tau} \boldsymbol{\tau} \bullet \delta\mathbf{x}\, d\Gamma = 0 \quad (5)$$

Next, a constitutive model needs to be specified for $\boldsymbol{\sigma}$. In the current simulations, we utilize the standard Newtonian liquid constitutive model, given by

$$\boldsymbol{\sigma} = -p\mathbf{I} + 2\mu\boldsymbol{\varepsilon}, \quad (6)$$

where p is the pressure, I is the identity tensor, μ is the dynamic viscosity, and ε is the strain rate tensor. Note that the appearance of a pressure term in the constitutive model is a result of the kinematic constraint of incompressibility. This incompressibility constraint typically presents a challenge in computational mechanics, particularly for finite elasticity and fluid mechanics simulations. Note that a non-Newtonian or viscoelastic constitutive model could be incorporated in place of Equation (6).

For fluid mechanics simulations invoking incompressibility, there are two general approaches for computing pressure. One method is to combine the momentum equations with mass conservation to derive a Poisson equation for pressure. An alternate method, referred to as artificial compressibility, utilizes an equation of state to relate pressure to volume dilatation. The use of artificial compressibility affects the unsteady portion of the Navier-Stokes equation, leaving the steady-state solutions independent of the sound speed (as long as a solution is obtained). This fact is often used to modify the sound speed for optimization of numerical convergence. However, when time-accurate solutions are required, care must be taken in choosing the sound speed. These methods are also referred to as penalty methods.

In the current work, we implemented a penalty-type approach in which pressure was related to volume dilatation according to

$$p = -K\left(\frac{V}{V_o} - 1\right) \quad (7)$$

where K is the bulk modulus and V/V_o is the relative volume.

The domain was discretized into quadrilateral finite elements and standard bilinear shape functions were used for interpolation. All integrals were performed using four-point Gaussian quadrature with the exception of the pressure term, on which one-point quadrature was used to maintain numerical stability.

Temporal integration was accomplished using an explicit, central-difference method,

$$\ddot{\mathbf{u}} = \frac{\mathbf{u}^{n+1} + \mathbf{u}^{n-1} - 2\mathbf{u}^n}{\Delta t^2} \quad (8)$$

$$\mathbf{a}^n = \ddot{\mathbf{u}}^n = \mathbf{M}^{-1}\mathbf{P}^n, \quad (9)$$

$$\mathbf{u}^{n+1} = \mathbf{M}^{-1}\mathbf{P}^n \Delta t^2 + 2\mathbf{u}^n - \mathbf{u}^{n-1}. \quad (10)$$

Displacement and acceleration are denoted by $\mathbf{u}$ and $\mathbf{a}$; $\mathbf{F}$ represents the vector of internal and body forces and $\mathbf{M}$ is the mass matrix. We used the lumped form of $\mathbf{M}$, in which the mass of each element is equally distributed among its nodes, yielding a diagonal mass matrix and independent nodal equations.

For initial validation of the model, we ran a simple two-dimensional test case – horizontal motion of a container of fluid. The model and boundary conditions are illustrated in Figure 1 (left) and a plot of the deformed surface during the simulation in Figure 1 (right). Note the large surface deformation that is able to be handled with the current formulation. To validate our formulation, the same model was run using the commercial finite element package, LS-Dyna (Livermore Software Technology Company; Livermore, CA) and the results were compared. Plotted in Figure 2 is the vertical displacement at the left wall for both cases, showing excellent agreement.

4.3 Numerical Model: Adaptive Meshing

Once the base method was validated as shown above, we implemented a strategy to update the finite element mesh when it became distorted. In general, there are three steps

involved in this process: (1) re-mesh the domain, (2) interpolate the solution from old grid to the new grid, and (3) detect the segments that are on the boundary of the new grid. Once these steps are completed, the simulation resumes. A flowchart illustrating the overall flow of the code is shown in Figure 3.

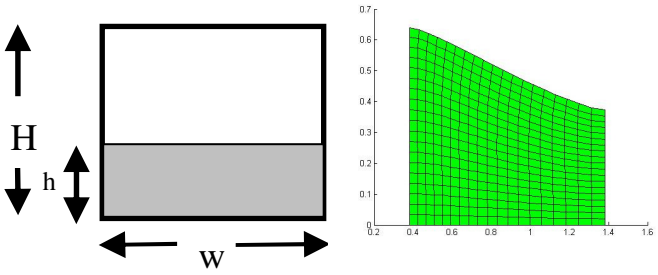

Figure 1: (left) Geometry for test problem (h=0.5 m, H=1.2 m, w=1 m). A 5 sec. load ramp was specified for the container horizontal velocity according to u=U(t/5), where *t* is time and U is the magnitude of the velocity. (right) Deformed shape during simulation.

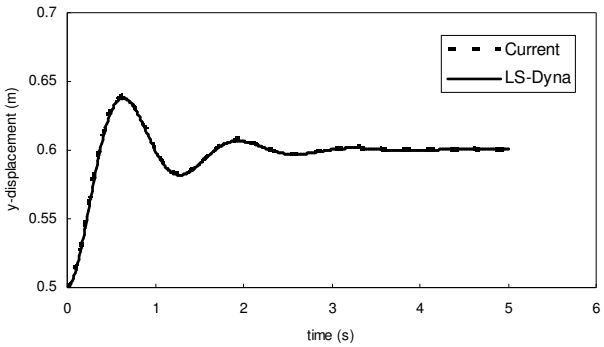

Figure 2: Vertical displacement at left wall for test case using current method and LS-Dyna, showing excellent agreement.

4.3.1 Re-mesh Step

While there are several excellent, open-source triangular mesh generators [4, 5], the automatic generation of purely quadrilateral meshes is not straightforward. In the current work, the pre-processor from the Abaqus finite element software package (Dassault Systèms, Providence, RI) was used to generate quadrilateral meshes. To accomplish this in an automated way, a python script (which is the scripting language utilized in Abaqus) was generated from the main simulation code. This script contained the boundary contour of the distorted mesh as well as the commands utilized in Abaqus to generate a quadrilateral mesh. Once the python script had been generated, a system call was issued from within the simulation code to execute the script within Abaqus. In this way, no user input was required to perform the re-mesh step.

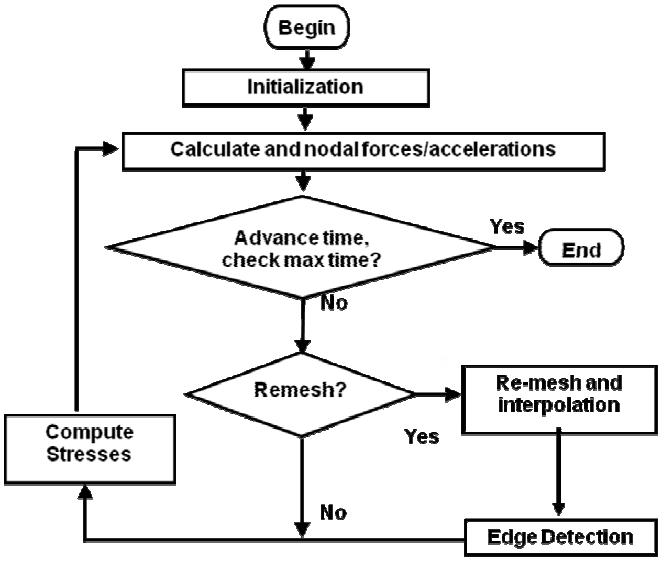

Figure 3: Flow chart showing overall simulation algorithm.

4.3.2 Interpolation Step

In this section, we will be considering two finite element meshes – the original mesh before the re-mesh has occurred (termed the *original mesh*) and the mesh after the re-mesh has occurred (referred to as *new mesh*). Note that these two meshes are associated with the same physical geometry and thus share the same boundary. This is illustrated in Figure 4.

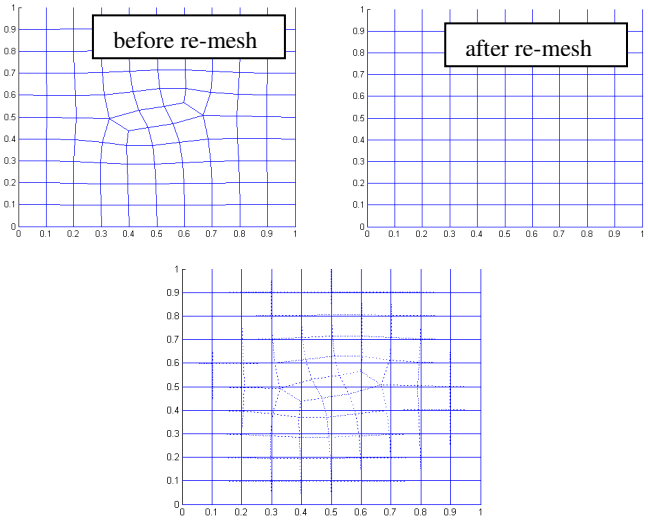

Figure 4: Example finite element meshes before (upper left) and after (upper right) a re-mesh step. The lower image has the meshes superimposed on one another.

In our simulation, the solution variables consist of the fluid velocities in the x and y direction. These variables are defined at the nodes of the finite element mesh. Note from Figure 4 that the nodes in the new mesh are generally not in the same location as the nodes of the original mesh. Thus, it is necessary to estimate the fluid velocity at each node of the new mesh, based on interpolating values from the original mesh.

To perform the interpolation for a given node in the new mesh (gray node in Figure 5), we first identify the element from the original mesh that contains this node (the element outlined in Figure 5).

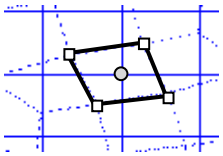

Figure 5. Schematic describing interpolation procedure. The original and new meshes are shown with dashed and solid lines.

Once the appropriate element in the original mesh has been identified, it is further divided into two triangles, and the triangle containing the node to be interpolated is identified. The three nodes of this triangle are then used to interpolate the nodal value in the new mesh using *barycentric coordinates* according to the formula [6]:

$$f = \frac{A_A}{A} f_A + \frac{A_D}{A} f_D + \frac{A_C}{A} f_C \qquad (11)$$

where A represents the area of the triangle, and f is the function to be interpolated at the point denoted by the red square. A_A, A_B, and A_D are areas the smaller triangles defined in Figure 7, below.

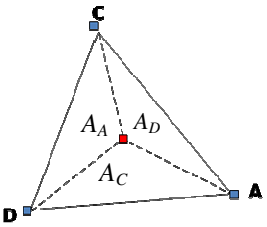

Figure 6. Definition of areas used for interpolation of nodal values.

4.3.3 Edge Detection Step

Finally, once the new grid has been constructed and solution variables interpolated, it is necessary to identify which nodes in the new mesh are on the boundary of the domain, and which are in the interior of the domain. This is necessary as the new nodes may have been inserted on the boundary, and knowledge of boundary nodes is necessary for proper enforcement of boundary conditions.

To detect whether a given node was a boundary or interior node, a simple algorithm was developed based on counting the number of elements attached to a given node. Note that this algorithm works only if the mesh is completely composed of quadrilateral elements and all elements are connected to each other at nodes.

As shown in Figure 7 (below), it was observed that any node attached to 1 element or 2 elements must be an edge node.

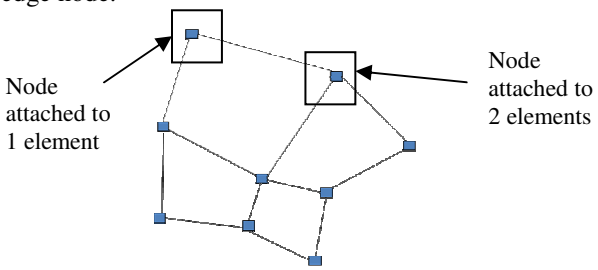

Figure 7. Example of element counting algorithm for nodes connected to 1 or 2 elements.

For nodes attached to three or more elements, it was observed that the following general principle governs whether a given node is a boundary or interior node. Let N be the number of nodes that the node in question is directly connected to through an element edge, and let E be the number of elements attached to the node. Then if $E=2N$ the node is an interior node and if $E=(2N+1)$ then it is a boundary node. This concept is illustrated below in Figure 8.

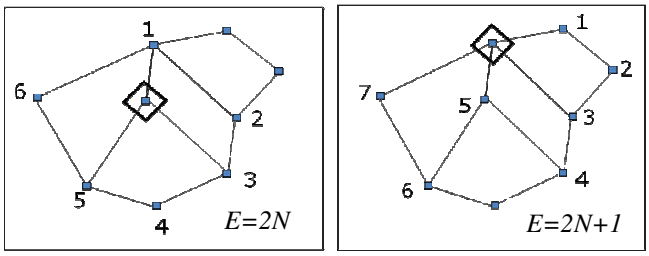

Figure 8. Example of element counting algorithm for nodes connected to 3 or more elements.

4.3.4 Validation

Once the preceding algorithms had been developed, implemented, and tested, they were incorporated into the main simulation code. To test the robustness of this method, we ran three simulations using the sloshing tank model described in the previous section. Cases were run with one re-mesh, three re-meshes, and the baseline case of

no re-meshes. Figure 9 below shows that the vertical fluid displacement at the left wall, which is indistinguishable for the three cases. This implies that the re-meshing and interpolation algorithms have not significantly degraded the solution.

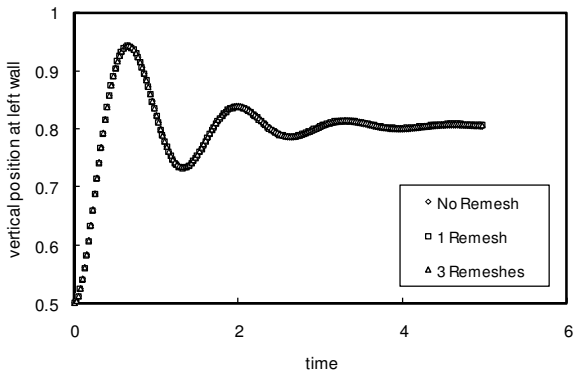

Figure 9. Validation runs for full simulation including re-meshing algorithms.

5. Experimental Studies

Once the model described in the previous section was validated against the simple test case, we sought to develop an experimental apparatus that could provide direct validation of the model predictions in a system that more closely resembled the oropharynx. In this section, we will discuss the design of the apparatus, as well as some preliminary tests conducted.

5.1 Experimental model

The experimental model consists of a fluid bolus contained in the central groove of a simulated tongue (Figure 10, below). The tongue model was housed in a transparent plastic casing, allowed visual access to fluid motions during the experiments. Dimensions of the model were estimated based on scaling data from the biplane videofluoroscopic study of Kahrilas et al.[7].

The tongue model was perturbed with upward and downward motions of various amplitudes, simulating pre-swallow lingual gestures, and the presence or absence of spillage recorded.

Figure 10. Experimental apparatus to study oropharyngeal fluid mechanics.

5.2 Fluids utilized

In addition to testing water, Thicken-Up powder thickener was added to vary liquid consistency. Nectar, honey, and pudding mixtures were prepared according to the manufacturer directions and tested.

Rheological properties for each liquid were determined using a Brookfield concentric-cylinder viscometer (Brookfield Engineering, Middleboro, MA). Temperature was maintained at 20° C using a temperature-controlled water bath and the Brookfield small sample adapter with temperature-control jacket. Fluids were tested for 5 minutes at a shear rate of 35 s^{-1}, with viscosity measurements acquired every 10 seconds. Each fluid was tested twice, and two different mixtures of each consistency were tested (for a total of 4 tests per consistency). Representative viscosity vs. time data for nectar and honey consistencies are shown below. Note that the initial viscosity decreases by almost a factor of two by the end of the test. This behavior was observed for all samples.

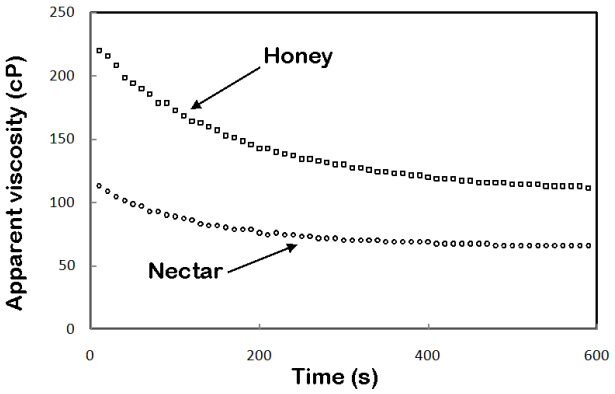

Figure 11. Viscosity vs. Time for nectar and honey liquids tested in this study.

5.3 Experimental Method

A prescribed volume of liquid (75 or 100 mL) was first loaded into the apparatus. With the back of the model constrained, the front edge was lifted a prescribed height (2, 4, 6, 8, or 10 cm), held for an instant, and then released. When bottom of the model hit the bench, the liquid moved forward, potentially spilling out the front of the model. The presence or absence of spillage was noted. Two trials of each height and consistency were performed on different days (investigators were blinded to the results while performing the tests). All trials were recorded on video for later analysis. Representative trials showing the absence and presence of spill are shown in Figure 7.

As shown below in Table 1, for small amplitude perturbations, all liquids were contained with no spillage. For moderate perturbations, un-thickened water spilled, while all thickened liquids were contained in the model.

For the largest perturbations studied, only the pudding-thick material did not spill.

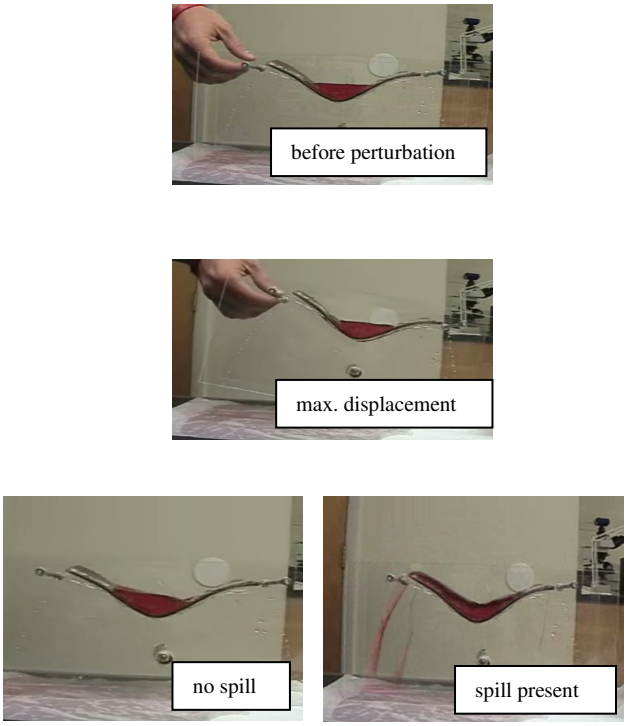

Figure 12. Representative trials, showing the absence and presence of spill.

	75 mL			100 mL		
Height (cm)	Nectar	Honey	Pudding	Nectar	Honey	Pudding
2	N	N	N	N	N	N
4	N	N	N	N	N	N
6	N	N	N	N	N	N
8	Y	N	N	Y	N	N
10	Y	Y	N	Y	Y	N

Table 1. Results of experimental trials shown presence or absence of spillage for different bolus volumes, consistencies, and drop heights.

6. Conclusions and Future Directions

We have presented a Lagrangian method with adaptive re-meshing to simulate the large-deformation free-surface flow fluid mechanics behaviour. The model has been validated against a simple "sloshing tank" problem. In addition, an experimental apparatus has been developed to validate the model which is physiologically relevant to swallowing mechanics.

Current work is focused on combining these two aspects of the project by developing a computer model of the experimental apparatus and solving the fluid mechanics. Once this has been accomplished, we will be able to assess the accuracy of the numerical model and apply it to study the fluid mechanics of oropharyngeal bolus transport.

7. Acknowledgments

The project described was supported by Grant Number 1R15DK079284 from the National Institute of Diabetes and Digestive and Diseases (NIDDK). Its contents are solely the responsibility of the authors and do not necessarily represent the official views of NIDDK or NIH.

References

[1] W.M. Lai, D. Rubin, and E. Krempl. *Introduction to Continuum Mechanics*, New York: Pergamon Press, 1993.

[2] D.J. Benson. "Computational methods in Lagrangian and Eulerian hydrocodes," *Comp. Meth. Appl. Mech. Engr.,* vol. 99, no2-3, pp. 389-405, 1992.

[3] T.J.R. Hughes. *The Finite Element Method: Linear Static and Dynamic Analysis*, Englewood Cliffs, NJ: Prentice Hall, 1987.

[4] Shewchuk J.R. "Delaunay refinement algorithms for triangular mesh generation," *Computational Geometry: Theory and Applications,* vol. 22, no 1-3, pp. 21-74, 2002.

[5] P.-O. Persson and G. Strang. "A simple mesh generator in Matlab," *SIAM Review,* vol 46, no 2, pp.329-345, 2004.

[6] T.R. Chandrupalta and A.D. Belegundu. *Introduction to Finite Elements in Engineering,* Englewood Cliffs, NJ: Prentice Hall, 1991.

[7] P.J. Kahrilas, S. Lin, J.A. Logemann, G.A. Ergun, and F. Facchini. "Deglutitive tongue action: Volume accommodation and bolus propulsion," *Gastroenterol.,* vol 104, pp. 152-162, 1993.